Eur. J. Biochem. **271**, 1497–1507 (2004) © FEBS 2004 doi:10.1111/j.1432-1033.2004.04057.x

Thermodynamic analysis of the unfolding and stability of the dimeric DNA-binding protein HU from the hyperthermophilic eubacterium *Thermotoga maritima* and its E34D mutant

Javier Ruiz-Sanz[1], Vladimir V. Filimonov[1,2], Evangelos Christodoulou[3], Constantinos E. Vorgias[3] and Pedro L. Mateo[1]

[1]*Department of Physical Chemistry, Faculty of Sciences and Institute of Biotechnology, University of Granada, Spain;* [2]*Institute of Protein Research, Russian Academy of Sciences, Pushchino, Moscow, Russia;* [3]*Faculty of Biology, Department of Biochemistry and Molecular Biology, National and Kapodistrian University of Athens, Greece*

We have studied the stability of the histone-like, DNA-binding protein HU from the hyperthermophilic eubacterium *Thermotoga maritima* and its E34D mutant by differential scanning microcalorimetry and CD under acidic conditions at various concentrations within the range of 2–225 μM of monomer. The thermal unfolding of both proteins is highly reversible and clearly follows a two-state dissociation/unfolding model from the folded, dimeric state to the unfolded, monomeric one. The unfolding enthalpy is very low even when taking into account that the two disordered DNA-binding arms probably do not contribute to the cooperative unfolding, whereas the quite small value for the unfolding heat capacity change (3.7 $kJ{\cdot}K^{-1}{\cdot}mol^{-1}$) stabilizes the protein within a broad temperature range, as shown by the stability curves (Gibbs energy functions vs. temperature), even though the Gibbs energy of unfolding is not very high either. The protein is stable at pH 4.00 and 3.75, but becomes considerably less so at pH 3.50 and below, to the point that a simple decrease in concentration will lead to unfolding of both the wild-type and the mutant protein at pH 3.50 and low temperatures. This indicates that various acid residues lose their charges leaving uncompensated positively charged clusters. The wild-type protein is more stable than its E34D mutant, particularly at pH 4.00 and 3.75 although less so at 3.50 (1.8, 1.6 and 0.6 $kJ{\cdot}mol^{-1}$ at 25 °C for $\Delta\Delta G$ at pH 4.00, 3.75 and 3.50, respectively), which seems to be related to the effect of a salt bridge between E34 and K13.

Keywords: differential scanning microcalorimetry; hyperthermophilic HU protein; polar interactions; thermal stability; unfolding heat capacity.

Proteins from thermophilic and hyperthermophilic microorganisms are of major interest to industrial biotechnology because they are usually more stable at high temperatures than their analogues from mesophilic organisms whilst they retain the folding patterns of their protein family [1–4]. Most attempts at discovering the origin of their stability have involved comparative thermodynamic and/or amino acid sequence analyses of homologous proteins from organisms living at different temperatures [1,2,5–9]. Thus it is generally accepted that to arrive at a complete understanding of the thermal adaptation strategies of these proteins it is necessary to obtain and compare the unfolding thermodynamic functions of mutants and other family members.

HU is a small histone-like bacterial protein that binds to DNA. It is abundant in all prokaryotes and its sequence is quite similar in a considerable number of species [10]. It is essential in the assembly of supramolecular nucleoprotein complexes and is also involved in a variety of DNA metabolic events, such as replication, transcription and transposition [11,12]. Its ability to repair DNA [13,14] and to prevent DNA duplex melting [7] has also been described.

HU proteins from several species of bacillus growing in environments of different temperatures have already been isolated and studied [4,7,15–18]. The close sequence homology among them suggests that their native structure must be very similar to a general pattern. The most extensively characterized thermophilic HU is the protein from *Bacillus stearothermophilus* (HU*Bst*), which consists of two identical polypeptide chains of 90 amino acid residues with a total molecular mass of 19.5 kDa. Not only has its three-dimensional structure been resolved by X-ray crystallography and NMR [19–21] (Fig. 1), but several mutational analyses have been made [4,22–24] to find out more about the contribution of certain key amino acids to its thermostability. A new HU protein from the extreme thermophile *Thermotoga maritima* (HU*Tmar*) has recently been purified and characterized

Correspondence to P. L. Mateo, Department of Physical Chemistry, Faculty of Sciences, University of Granada, 18071 Granada, Spain. Fax: + 34 958 272879, Tel.: + 34 958 243333,
E-mail: pmateo@ugr.es

Abbreviations: HU*Tmar*, DNA-binding protein HU from *Thermotoga maritima*; HU*Bst*, DNA-binding protein HU from *Bacillus stearothermophilus*; E34D, single mutant of HU*Tmar* with glutamic acid 34 replaced by aspartic acid; T_m, temperature at which the fraction of the folded dimer equals the fraction of the unfolded monomer; T_g, T_h and T_s, temperatures at which the unfolding $\Delta G(T)$, $\Delta H(T)$ and $\Delta S(T)$ equal zero, respectively; DSC, differential scanning microcalorimetry. A website is available at http://www.ugr.es/local/qmfisica/

(Received 10 November 2003, revised 18 February 2004, accepted 26 February 2004)

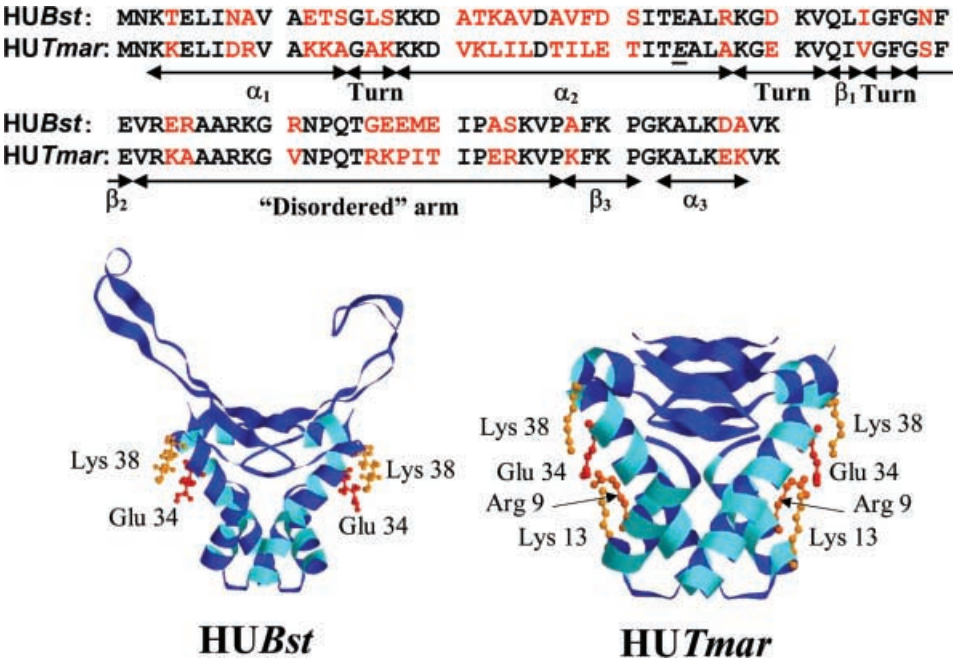

Fig. 1. Structural models of HU proteins from *B. stearothermophilus* [20] and *T. maritima* [18]. The upper part of the figure shows the aligned amino acid sequences of each monomer within the homodimers, the ribbon models of which are shown in the lower part. The nonconserved positions within the sequences are shown in red whilst the mutation point within HU*Tmar* (E34) is underlined. Some positively charged side chains surrounding this residue are shown in ball-and-stick form on the three-dimensional models.

[4,7,17,18]. Its three-dimensional structure is very similar to that of the HU*Bst* protein: the homodimer forms a compact body, including several intertwined α-helices, a pair of triple-stranded β-sheets and two 'disordered arms', which are quite flexible in the absence of DNA and not very clearly defined in the X-ray picture of the protein (Fig. 1).

We report here the results of an extensive thermal-stability study of a hyperthermophilic protein, the histone-like protein from *T. maritima* (HU*Tmar*-wt) and its E34D mutant, carried out using differential scanning microcalorimetry (DSC) and CD spectroscopy. The combination of these two techniques allowed us to determine the thermodynamic parameters of the native, dimeric structure and its thermal unfolding, and to describe some of the experimental and mathematical bases for future studies into strategies for increasing the thermal stability of proteins.

Materials and methods

Overproduction and purification of HU proteins

Wild-type HU protein from *T. maritima* (HU*Tmar*-wt) and its mutant E34D (HU*Tmar*-E34D) were overproduced and purified as described previously [4,17]. Protein samples were checked for homogeneity by SDS/PAGE and gel filtration on a Superdex 75 analytical column. Before all experiments, the samples were dialyzed overnight against a buffer of sodium acetate (50 mM, pH 4.00 and 3.75) or glycine (50 mM, pH 3.50) as appropriate.

Protein concentration was measured spectrophotometrically at 257 nm using a value of 600 $M^{-1}\cdot cm^{-1}$ for the extinction coefficient, determined by the method of Gill & von Hippel [25]. The samples were dialyzed at high concentration to obtain suitable optical density values and were then diluted to experimental concentration. All molar quantities and calculations throughout this paper are given in terms of mols of monomer.

DSC measurements

DSC was performed on a VP-DSC microcalorimeter (MicroCal) at a heating rate of 1.5 $K\cdot min^{-1}$ using protein concentrations within the range 0.3–2.2 $mg\cdot mL^{-1}$. The partial molar heat capacity was calculated assuming 0.73 $mL\cdot g^{-1}$ for the partial specific volume, and 9.99 kDa and 9.98 kDa for the molecular masses of HU*Tmar*-wt and E34D, respectively. After transforming the DSC traces into partial molar heat capacity curves, they were subject to single and multiple fitting procedures using ORIGIN 4.1 software from MicroCal. User-designed procedures based on the equations corresponding to the equilibrium model

$$\frac{1}{2}N_2 \longleftrightarrow U \qquad \text{Eqn (1)}$$

were also used. To approximate the baselines of the DSC curves, i.e. the temperature dependence of the heat capacity of the initial and final conformations ($C_{p,N2}$ and $C_{p,U}$), the heat capacity of the native state was taken to be a linear function of temperature and that of the unfolded state to be a quadratic function [26].

The two-state dissociation/unfolding model

The two-state model (Eqn 1) was used for the analysis of DSC and CD unfolding curves. All the equations and thermodynamic parameters in this paper are given in terms

of mols of protein monomer. At any given total protein concentration, C_t, the molar fractions of the polypeptide chains forming the native dimer (X_{N2}), the unfolded monomer (X_U) and the equilibrium constant (K_U) can be presented as:

$$X_{N2} = 2[N_2]/C_t \quad \text{Eqn (2)}$$

$$X_U = [U]/C_t \quad \text{Eqn (3)}$$

$$K_U = [U]/[N_2]^{1/2} \quad \text{Eqn (4)}$$

As $X_{N2} + X_U = 1$, K_U can be expressed as:

$$K_U = X_U \cdot \left(\frac{2C_t}{1-X_U}\right)^{\frac{1}{2}} \quad \text{Eqn (5)}$$

Simple transformation of this equation leads to:

$$X_U = \left(\frac{K_U}{4C_t}\right) \cdot \left(-K_U + \sqrt{K_U^2 + 8C_t}\right) \quad \text{Eqn (6)}$$

The enthalpy of the system will be:

$$\langle H \rangle = X_{N2} \cdot H_{N2} + X_U \cdot H_U = (1 - X_U) \cdot H_{N2} + X_U \cdot H_U = H_{N2} + X_U \cdot \Delta H_U \quad \text{Eqn (7)}$$

where ΔH_U is the unfolding enthalpy change, that is, H_U–H_{N2}.

The derivative of this expression with respect to temperature at a constant pressure gives the heat capacity of the protein, C_p:

$$C_p = \frac{d\langle H \rangle}{dT} = \frac{dH_{N2}}{dT} + X_U \cdot \frac{d\Delta H_U}{dT} + \Delta H_U \cdot \frac{dX_U}{dT} \quad \text{Eqn (8)}$$

Derivation of Eqns (5) or (6) leads to the value of dX_U/dT:

$$\frac{dX_U}{dT} = \frac{dK_U}{dT}\left[\frac{2X_U(1 - X_U)}{K_U(2 - X_U)}\right] \quad \text{Eqn (9)}$$

and using the van't Hoff expression $\frac{dK_U}{dT} = \frac{K_U \Delta H_U}{RT^2}$ we obtain

$$\frac{dX_U}{dT} = \frac{2X_U(1 - X_U) \cdot \Delta H_U}{(2 - X_U) \cdot R \cdot T^2} \quad \text{Eqn (10)}$$

The change of ΔH_U with temperature corresponds to $\Delta C_{p,U}$, the heat capacity change upon unfolding, i.e. $\Delta C_{p,U} = C_{p,U} - C_{p,N2}$, where $C_{p,N2}$ and $C_{p,U}$ stand for the molar heat capacities of the native and unfolded states, respectively; that is, the changes of H_{N2} and H_U with temperature. Substitution of this and Eqn (10) in Eqn (8) produces the equation for the molar heat capacity of the system as a function of temperature, i.e. during the DSC scan:

$$C_p = C_{p,N2} + X_U \cdot \Delta C_{p,U} + \frac{2\Delta H_U^2 \cdot X_U \cdot (1 - X_U)}{(2 - X_U) \cdot R \cdot T^2} \quad \text{Eqn (11)}$$

The equilibrium constant, K_U, is expressed in terms of the Gibbs energy change as

$$K_U(T) = \exp(-\Delta G_U(T)/R \cdot T) \quad \text{Eqn (12)}$$

where

$$\Delta G_U(T) = \Delta H_U(T) - T \cdot \Delta S_U(T) \quad \text{Eqn (13)}$$

whilst $\Delta H_U(T)$ and $\Delta S_U(T)$ are the changes in enthalpy and entropy, respectively.

In Eqn (1) the concentration-dependent transition midpoint, T_m, might be defined as the temperature where $X_N = X_U = 0.5$, whilst T_g, T_h and T_s stand for the temperatures at which $\Delta G_U(T_g)$, $\Delta H_U(T_h)$ and $\Delta S_U(T_s)$ equal zero, respectively. The unfolding enthalpy and entropy functions can then be written in terms of T_m as:

$$\Delta H_U = \Delta H_{U,m} + \int_{T_m}^{T} \Delta C_{p,U} \cdot dT \quad \text{Eqn (14)}$$

$$\Delta S_U = \Delta S_{U,m} + \int_{T_m}^{T} \frac{\Delta C_{p,U}}{T} \cdot dT \quad \text{Eqn (15)}$$

As Eqn (5) leads to $K_{U,m} = (C_t)^{1/2}$ at T_m, by combining Eqns (12) and (13) we get ΔG_U at T_m as

$$\Delta G_{U,m} = \Delta H_{U,m} - T_m \cdot \Delta S_{U,m} = -R \cdot T_m \cdot \ln(C_t)^{\frac{1}{2}} \quad \text{Eqn (16)}$$

By using Eqn (16), Eqn (15) can be expressed in terms of $\Delta H_{U,m}$:

$$\Delta S_U = \frac{\Delta H_{U,m}}{T_m} + 0.5 \cdot R \cdot \ln(C_t) + \int_{T_m}^{T} \frac{\Delta C_{p,U}}{T} \cdot dT \quad \text{Eqn (17)}$$

To fit the experimental molar-heat-capacity curves to Eqn (11) we have assumed a linear temperature dependence for $C_{p,N2}$ and a quadratic one for $C_{p,U}$, as described elsewhere [26].

$$C_{p,N2} = a_N + b_N \cdot T \quad \text{Eqn (18)}$$

$$C_{p,U} = a_U + b_U \cdot T + c_U \cdot T^2 \quad \text{Eqn (19)}$$

Parameters b_U and c_U were obtained from the nonlinear quadratic regression via the $C_{p,U}$-values estimated from the amino acid content, as described elsewhere [27]. When fitting a single heat-capacity curve only two parameters, b_U and c_U, were fixed, whilst the other five parameters, T_m, $\Delta H_{U,m}$, a_N, b_N and a_U, were adjustable.

According to Eqn (1) protein concentration will only affect the T_m values, whereas other parameters and thermodynamic functions of temperature are common and remain unaffected by concentration. Therefore, for example, in order to fit simultaneously the curves recorded at four different concentrations (the multiple four-concentration curve fitting) the nonlinear regression program will adjust only one pair of parameters, T_m and $\Delta H_{U,m}$, for any selected reference concentration (we chose 120 μM of monomer arbitrarily), $C_{t,ref}$, in addition to the other three parameters mentioned above. A similar approach was used to fit the curves recorded at various pH values, as it was assumed that the unfolding enthalpy depends upon temperature alone and not on pH (Appendix).

CD measurements

CD measurements were made with a Jasco-715 spectropolarimeter (Japan) equipped with a PTC-348WI temperature control unit. Temperature scans were carried out at a heating rate of 1 K·min^{-1} using quartz cells with a 1 mm path. To check the reversibility of the unfolding process, CD spectra were recorded on three occasions: before starting the scans, at the highest possible temperature (usually 90 °C) and then again on cooling the sample to its initial temperature. To fit the CD thermal curves, all of the equations described for the DSC fittings are applicable, but here the data to be fitted corresponds to the ellipticity signal at 222 nm, θ_{222}, instead of C_p values:

$$\theta_{222} = \theta_{N2} + X_U \cdot (\theta_U - \theta_{N2}) \qquad \text{Eqn (20)}$$

In these fittings we have assumed linear temperature dependences of θ_{222} for both the native (θ_{N2}) and unfolded (θ_U) states:

$$\begin{aligned} \theta_{N2} &= \theta_{N2,a} + \theta_{N2,b} \cdot T \\ \theta_U &= \theta_{U,a} + \theta_{U,b} \cdot T \end{aligned} \qquad \text{Eqn (21)}$$

To carry out CD experiments at a fixed temperature and various protein concentrations the temperature of the samples within the cells was controlled by thermostat for 5 min before the spectra were measured. For each spectrum five scans from 250 to 200 nm were made at a scan rate of 50 nm per minute. The cell width was changed according to protein concentration: 2 mm between 2 and 14 μM, 1 mm between 10 and 45 μM, and 0.2 mm between 30 and 180 μM. For all the CD experiments, protein samples were prepared by diluting the same stock solutions as those used in the DSC experiments. To fit these data to Eqn (1) we have used the $K_{U,w}$-value at the working CD temperature, T_w, obtained by multiple DSC-curve fittings (Appendix).

Results

DSC

We studied the thermal unfolding of both the wild-type HU*Tmar* protein and its E34D mutant in acidic solutions (pH 4.00, 3.75 and 3.50) to improve the reversibility of unfolding and avoid postunfolding aggregation. Judging by the complete reproducibility of the calorimetric traces after cooling the sample within the DSC cell, the heat-induced unfolding was highly reversible under all conditions. As shown in Fig. 2, thermal stability depended greatly upon pH and the mutant was less stable than the wild-type protein. As might be expected, the T_m values of both proteins increased concomitantly with protein concentration (Fig. 3), indicating that the unfolding was accompanied by chain dissociation. To analyze this effect the DSC unfolding experiments were carried out with protein concentrations of from 30 to 225 μM of monomer (from 0.3 to 2.25 mg·mL^{-1}) at each pH value.

As it is currently accepted that native HU proteins are dimers (see [10] for a review), the simplest applicable model should be that of a two-state unfolding/dissociation process

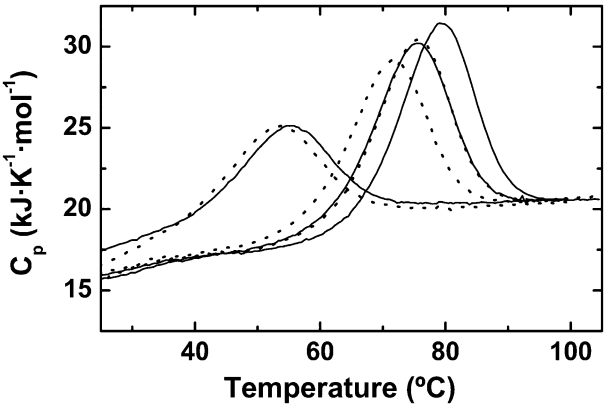

Fig. 2. Temperature dependence of the partial molar-heat capacity of the HU*Tmar* proteins at different pH values. Solid lines correspond to the wild-type HU*Tmar* and dotted lines to its E34D mutant. The pH values are 4.00, 3.75 and 3.50 from right to left. The monomer concentration is 120 μM in all cases.

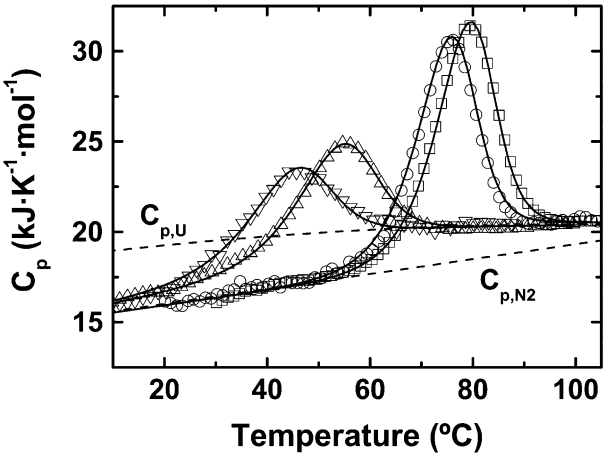

Fig. 3. Selected results of the multiple curve fitting for HU*Tmar*-wt. The heat capacity curves were recorded at various pH and concentration values: pH 4.00, 120 μM (□) and 30 μM (○); pH 3.50, 120 μM (△) and 30 μM (▽). Solid lines correspond to the best fittings to the two-state equilibrium model (Eqn 1). Dashed lines show the common temperature dependencies of the heat capacities of the native ($C_{p,N2}$) and unfolded ($C_{p,U}$) states obtained from the fittings.

(Eqn 1) in which only the native dimeric, N_2, and the unfolded monomeric, U, states are populated to any extent in solution. In fact, judging by the quality of the single-curve fittings (data not shown), each DSC curve follows this model quite well. Nevertheless, past experience suggests that a more appropriate way to analyze the DSC data would be via a multiple curve fitting [26], which, among other factors, would also take into account the effect of protein concentration. Because our studies were carried out in the acid pH range, where the heat effects of ionization are generally small and are also well compensated by the heat of proton transfer between the protein and the buffer, it is reasonable to assume that the heat capacities of both the native and unfolded states depend upon neither the pH nor the protein

concentration. If this should be the case both ΔH_U and $\Delta C_{p,U}$ should depend upon temperature alone, whilst ΔG_U will also be influenced by factors affecting the entropic component of the Gibbs energy, such as protein concentration or electrostatic contributions. Furthermore, as in the mutation only one exposed acidic group is replaced by another, it is also quite reasonable to assume that the heat capacities of both the wild-type protein and the mutant will coincide within the limits of experimental accuracy and therefore the heat-capacity change on unfolding will be the same for the wild-type and the mutant protein.

The quality of the multiple-curve fittings to Eqn (1) is indeed very good for both variants at all the concentrations and pH values studied (Fig. 3 and Table 1). Nevertheless, although the DSC curves recorded at pH 3.50 and even at pH 3.25 (data not shown) fit the model well under the assumptions mentioned above, at pH 3.50 and below both protein variants are only marginally stable and thus their thermal unfolding begins at room temperature, particularly at low concentrations. In addition, considering that at lower temperatures the unfolding heat approaches zero and therefore the thermal transitions widen, reliable DSC data for pH values lower than 3.75 were obtained only at relatively high monomer concentrations (120 μM and above).

As shown in Fig. 2, the E34D mutant is structurally less stable than the wild-type protein and, incidentally, its DSC curves recorded at pH 4.00 almost coincide with those of the wild-type protein at pH 3.75 at each concentration. This difference in stability, however, clearly decreases at pH 3.50 and eventually disappears when pH drops to 3.25, which should reflect the fact that the groups occupying position 34 in both protein variants are losing their charge close to pH 3 and no longer contribute to the energy balance.

As shown in Fig. 4, the multiple curve fittings result in a single unfolding enthalpy function, common to both protein variants for the three pH values and different concentrations assayed, which can be represented by the empiric equation:

$$\Delta HU(\mathrm{kJ\cdot mol^{-1}}) = 3.35(T - T_h) - 5.1\times10^{-2}(T - T_h)^2 - 6.0\times10^{-4}(T - T_h)^3 \qquad \text{Eqn (22)}$$

where T_h stands for the temperature at which ΔH_U equals zero (Materials and methods).

It should be noted that when the fitting parameters are not restricted (as occurs during individual curve fittings) the unfolding heats obtained at the corresponding T_m values practically coincide with the common enthalpy function (Fig. 4), which proves the validity of the two-state model and thus justifies the extrapolation of the unfolding Gibbs energies to 25 °C (Table 1).

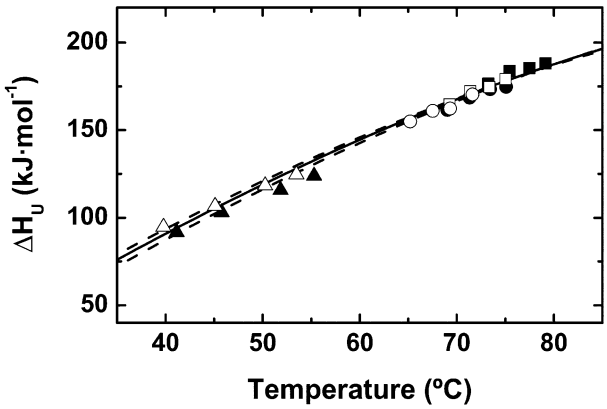

Fig. 4. The temperature dependence of the unfolding heat effect for the HU*Tmar* proteins. The solid line corresponds to the common $\Delta H_U(T)$ for HU*Tmar*-wt and its E34D mutant obtained from the multiple 24-curve fitting of DSC data to the two-state model. The dashed lines show the confidence interval of the fitting. The results of the individual curve fittings ($\Delta H_{U,m}$ vs. T_m) for both the wild-type protein (filled symbols) and the mutant (open symbols) at four different concentrations at the three pH values 4.00, 3.75 and 3.50 (■□, ●○ and ▲△, respectively) are also shown for comparison.

CD experiments

Because the globular-dimer core of the HU protein is highly α-helical, we also used far-UV CD to follow the thermal unfolding. This had the added advantage of allowing us to use a lower concentration range (180–2 μM of monomer) compared to that used in the DSC studies (225–30 μM). First of all we recorded far-UV CD spectra at different temperatures to reveal the spectral differences between the native and unfolded conformations (Fig. 5A). The spectra of the native states of the wild-type and mutant were found to be practically identical, corresponding to an α-helicity of about 41%, which coincides with the structural data. The spectra recorded at 90 °C are quite typical of an unfolded conformation, with a considerable change in the signal at 222 nm, confirming the loss of the α-helical content upon unfolding.

Table 1. Thermodynamic parameters of the heat-induced unfolding of HU*Tmar*-wt and its E34D mutant. Values were determined by the simultaneous fitting of 24 DSC curves (recorded at various pH and protein concentrations) to the two-state model (Eqn 1). The T_m and $\Delta H_{U,m}$-values refer to the transition midpoint at the monomer concentration of 120 μM. $\Delta G_{U,25}$ and $\Delta\Delta G_{U,25}$ stand for the changes in standard Gibbs energy at 25 °C ($\Delta G_{U,25}$) and their excess ($\Delta\Delta G_{U,25}$) above the $\Delta G_{U,25}$ of the E34D mutant. The T_g values refer to the condition $\Delta G_U(T_g) = 0$.

pH	HU*Tmar* variants	T_m (°C)	$\Delta H_{U,m}$ (kJ·mol^{-1})	$\Delta G_{U,25}$ (kJ·mol^{-1})	T_g (°C)	$\Delta\Delta G_{U,25}$ (kJ·mol^{-1})
4.00	Wild type	77.5 ± 0.2	183 ± 2	28.5 ± 0.3	101.9 ± 0.2	1.8 ± 0.3
	E34D	73.4 ± 0.2	175 ± 2	26.7 ± 0.3	98.0 ± 0.2	
3.75	Wild type	73.2 ± 0.2	174 ± 2	26.6 ± 0.3	97.8 ± 0.2	1.6 ± 0.3
	E34D	69.3 ± 0.2	166 ± 2	25.0 ± 0.3	94.2 ± 0.2	
3.50	Wild type	45.2 ± 0.3	106 ± 3	16.0 ± 0.4	74.4 ± 0.3	0.6 ± 0.4
	E34D	43.2 ± 0.3	100 ± 3	15.4 ± 0.4	73.0 ± 0.3	

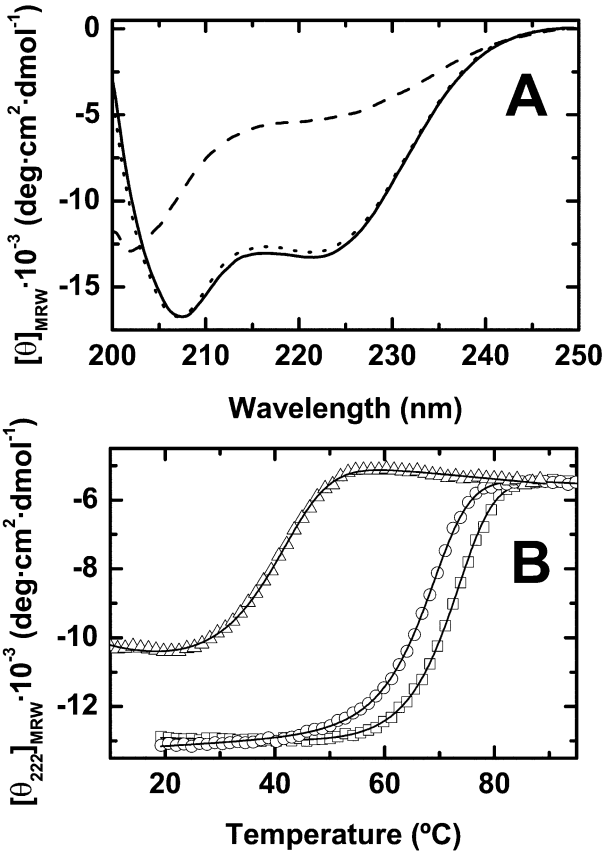

Fig. 5. CD experiments in the far-UV region of the HU*Tmar*-wt protein. (A) CD spectra in the far-UV region at pH 4.00 and different temperatures: 20 °C (—), 90 °C (- - -) and 20 °C once more, after cooling the heated sample (···). (B) Temperature dependencies of θ_{222} at three pH values (from left to right: 3.50, 3.75 and 4.00). Symbols correspond to experimental data, whilst solid lines show the individual best fittings to the two-state model. The monomer concentration in all experiments was 30 μM.

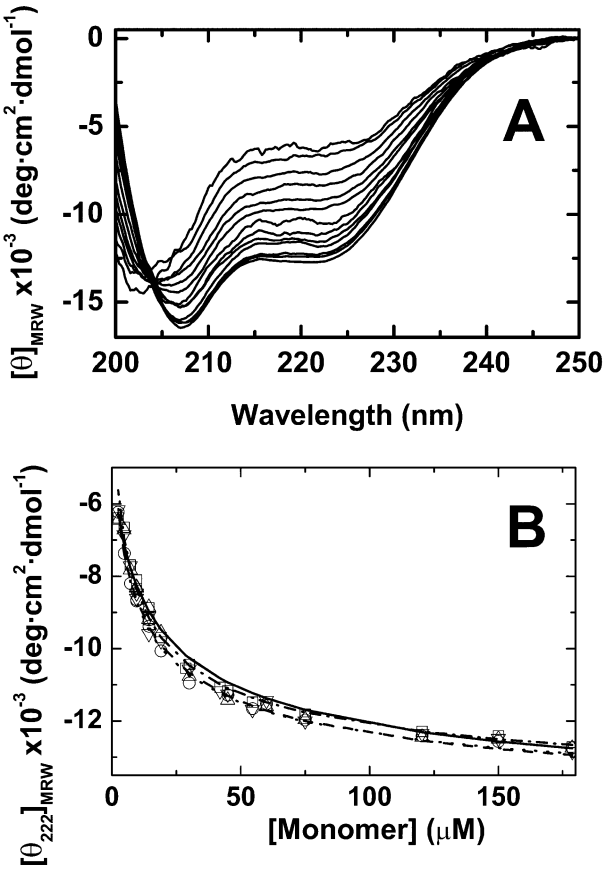

Fig. 6. Concentration dependence of the CD spectra in the far-UV range (A) and of θ_{222} (B) for the HU*Tmar*-E34D mutant at pH 3.50. The solid lines in (A) were recorded at 20 °C at the following monomer concentrations (from top to bottom): 2, 5, 7, 10, 15, 20, 30, 45, 60, 75, 120, 150 and 180 μM. The symbols in (B) correspond to various concentrations between 2 and 180 μM at four different temperatures: 10, 15, 20 and 25 °C (□, ○, △ and ▽, respectively). The four lines show the best nonlinear fittings to the equations of the two-state unfolding/dissociation model.

These changes are highly reversible as the spectra are completely restored after the heating/cooling cycle (Fig. 5A).

The temperature dependencies of θ_{222} for the wild-type and the E34D mutant proteins were recorded at pH 4.00, 3.75 and 3.50 at monomer concentrations of 15, 30 and 60 μM (Fig. 5B). It should be emphasized that the two latter concentrations were common to both the CD and DSC experiments, which allows a simultaneous fitting of the temperature dependencies of $\theta_{222}(T)$ and $C_p(T)$. It also allows us to check whether the thermodynamic parameters deriving from the DSC data accurately describe the temperature dependence of the θ_{222} values, which include concentrations well below the limits of DSC experiments.

Very good fittings of the CD data were obtained using the thermodynamic unfolding parameters set out in Table 1. This coincidence further confirms the validity of the two-state model (Eqn 1) as it adequately describes the temperature-induced unfolding curves independently of the observable used for monitoring the conformational changes.

As stated above, the native structure became highly unstable when pH was reduced to 3.50. From the CD melting curves (Fig. 5B) registered at the relatively low monomer concentration of 30 μM it can be seen that at around 20 °C (a value close to T_s, the temperature of maximum stability) the molar fraction of unfolded state was still about 0.2 and did not decrease any further at lower temperatures due to the proximity of the cold denaturation of the protein, that is to say, at this concentration and pH the protein molecules are never 100% folded at any temperature. In fact a further decrease in concentration to 2 μM at pH 3.50 results in an almost complete unfolding of the native structure at room temperature (Fig. 6A). The existence of an isosbestic point at about 204 nm suggests once more that the changes in CD spectra reflect the existence of an equilibrium between two protein conformations, the native dimer and the unfolded monomer, as predicted by the two-state model (Fig. 6A). This conclusion is confirmed by the fact that the concentration dependencies of CD at a fixed wavelength and different temperatures quantitatively follow the functions predicted by the model (Fig. 6B).

Discussion

DSC and CD data analyses show that in acidic solutions (pH 3.5–4.0) the heat-induced unfolding of both variants of HU*Tmar* strictly obeys the two-state dissociation/unfolding model (Eqn 1). The multiple DSC curve fittings made under the assumption of common, pH-independent $C_{p,N}$, $C_{p,U}$ and ΔH_U values provide a consistent set of thermodynamic parameters which correctly predict the concentration dependence of T_m, and allow us to extrapolate the standard Gibbs energy changes at each pH value throughout the whole experimentally accessible temperature range.

Thermodynamic stability of proteins is best characterized by the function $\Delta G_U(T)$ and it has been reasoned that the increased stability of thermophilic proteins may be put down to one or more of three different mechanisms [1,28]: (a) a shift in the $\Delta G_U(T)$ stability curve towards higher temperatures; (b) a rise in the Gibbs energy values, mostly because of an increase in its enthalpic contribution; and (c) a decrease in $\Delta C_{p,U}$, which results in a flatter, wider stability curve.

Fig. 7 shows that maximum ΔG_U for both HU*Tmar* variants appears at around 20 °C, a temperature similar to or lower than the corresponding ones for other nonthermophilic proteins. Therefore, there seems to be no shift in the stability curve with the hyperthermophilic HU*Tmar* protein.

The average specific enthalpy of unfolding for globular proteins was proposed by Privalov [10] to be around 50 J·g^{-1} at 110 °C. This specific enthalpy for HU*Tmar* at 110 °C is only about 23 J·g^{-1}, which is much lower than that proposed by Privalov. The simplest explanation might arise from the fact that HU proteins have long 'unstructured' arms (Fig. 1), which in all probability do not contribute to the overall heat effect of the co-operative unfolding. Nevertheless, elimination of the contribution of residues 52–86 (the positions of which are not defined by X-ray crystallography in HU*Tmar*) to the molecular mass, leads to only 38 J·g^{-1} for the specific enthalpy of unfolding of the structured protein core at 110 °C, still a lower value than Privalov's 50 J·g^{-1}. It should be noted here, however, that this is not the first case in which the high thermal stability of a globular protein is accompanied by low specific unfolding enthalpies; a recently reported example is that of the nonthermophilic, though extremely stable, enterocin AS-48 [30]. Another such example might be that of the hyperthermophilic cold-shock protein from *T. maritima* [31], which has a significantly lower unfolding enthalpy than its mesophilic homologues and where entropy factors seem to play the most important role in stabilization (see below). Hence the conclusion arrived at elsewhere [32] that a large unfolding enthalpy at high temperature might constitute an important factor in providing high thermostability to the native structure does not seem to apply to the HU*Tmar* protein, which, anyway does not have a particularly high $\Delta G_U(T_s)$ value either (Fig. 7).

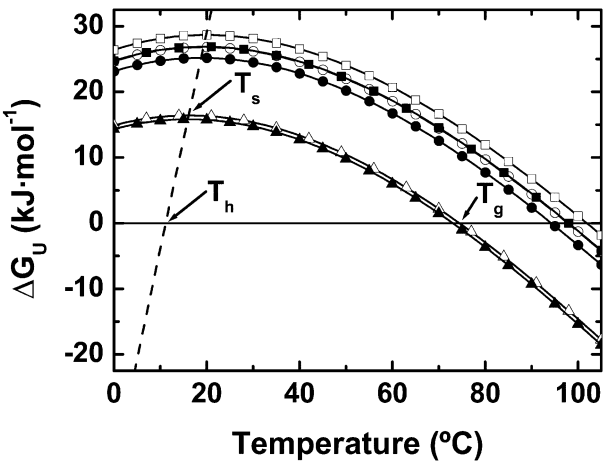

Fig. 7. Profiles of the standard Gibbs energy of unfolding for the HU*Tmar* proteins. HU*Tmar*-wt (open symbols) and its E34D mutant (filled symbols) at pH 4.00 (□,■), 3.75 (○,●) and 3.50 (△ ▲). Note that the stability curve of the wild-type protein at pH 3.75 practically coincides with that of the mutant at pH 4.00. The dashed line corresponds to the common unfolding enthalpy function (Eqn 22 and Fig. 4), which crosses the $\Delta G_U(T)$ lines at the corresponding T_s values, i.e. at temperatures at which ΔG_U reaches the maximum under each condition. T_h is common for all conditions, whilst the values of T_g and T_s are indicated as an example for the wild-type protein at pH 3.50.

$\Delta C_{p,U}$ defines the curve of the protein-stability graph and has proved to be an important parameter in thermal stability [1,28,32]. For example, simulations show that the smaller the $\Delta C_{p,U}$ the wider the $\Delta G_U(T)$ curve and thus the higher the melting point, T_g, for a given Gibbs energy maximum, $\Delta G_U(T_s)$ [32,33]. This effect is shown in Fig. 7 for both the wild-type and the HU*T*mar mutant, where T_g reaches around 100 °C when pH is equal to or above 3.75. In fact, the $\Delta C_{p,U}$ found at 25 °C (3.17 kJ·K^{-1}·mol^{-1} or 0.32 J·K^{-1}·g^{-1}) is a comparatively small value and also somewhat lower than the heat-capacity change estimated for this protein by the empirical algorithms proposed elsewhere [34], which appears then to justify the high thermal stability of the protein. This experimental finding has very recently been predicted on theoretical grounds in the literature [35,36], suggesting that the tendency for a reduced $\Delta C_{p,U}$ in thermophilic proteins is related to enriched polar interactions. Furthermore, as $\Delta C_{p,U}$ results largely from alterations in the hydration of hydrophobic and hydrophilic residues upon unfolding due to changes in the water-exposed surfaces, it would be reasonable to expect these changes to be similar for HU*Bst* and HU*Tmar*, which would imply that their $\Delta C_{p,U}$ values should also be similar, a conclusion still to be checked experimentally by measuring the heat effect of HU*Bst* unfolding. In this case, the higher stability of HU*Tmar* compared to that of HU*Bst* would not result from the curvature of the $\Delta G_U(T)$ function but from its magnitude, caused by the known entropic contribution of electrostatic interactions. A precisely similar situation is shown in Fig. 7, where for the same $\Delta C_{p,U}$ we can see a decrease between the $\Delta G_U(T)$ values of the wild-type and the mutant at each pH, as well as an overall decline in these values as pH descends from pH 4.00 to 3.50, which in both cases is concomitant with a decrease in charged residues and electrostatic interactions (see below).

A comparison of the unfolding data between the HU*Tmar*-wt protein and its E34D mutant shows that

the single amino acid replacement destabilizes the native structure of the protein by about 1.8 kJ·mol^{-1} at pH 4.00 and 25 °C in terms of the standard Gibbs energy change (Table 1). In fact, Glu34 has been proposed to be one of the three key residues, together with Gly15 and Val42, responsible for the high thermostability of HU*Bst* [22–24] and particularly of HU*Tmar* compared to their mesophilic counterparts [4,18]. An inspection of the three-dimensional structure of the wild-type protein (Fig. 1) reveals the existence of a salt bridge between Glu34 in one chain and Lys13 in the other [18], an interaction that cannot take place in HU*Bst* as there is a Thr at position 13 (Fig. 1). It is tempting therefore to surmise that this salt bridge, which breaks down upon substituting Asp for Glu [18], may well be at least partially responsible for the higher stability of the wild-type protein compared to the mutant. Thus, the value of 1.8 kJ·mol^{-1} could be taken as being the maximum cost of the disruption of the K13-E34 salt bridge at pH 4.00.

Nevertheless, there is no commonly held view in the literature on the energetic advantages of solvent-exposed salt bridges as the disruption of a salt bridge by the substitution of one of the partners by a neutral amino acid does not always decrease the stability of the original structure [2]. A more comprehensive view emerges that an important effect on stability at high temperatures might derive from charge clustering and electrostatic networks on the protein surface [18,37], although uncompensated charge repulsion tends to increase the Gibbs energy of the native conformation, thus decreasing its stability. Some metal-binding proteins, such as parvalbumins, present the classic example of the removal of strongly bound cations causing an enormous destabilization of the folded conformation, which leads to an uncompensated charge repulsion within the binding sites [38]. Nevertheless, it must be noted here that the function of histones is to bind and pack the highly charged DNA and thus the high positive charge on the surface of HU's may play a role not only in their stability but also in promoting a better interaction with DNA and other neighbors, particularly at high temperatures in the case of thermophilic and extremely thermophilic proteins.

It would appear then that the considerable excess of positive charge in HU*Tmar* (+16 vs. +4 for HU*Bst*), which is at least partially compensated at neutral pH by the evenly distributed acid groups, could well play a role in the high melting temperature of the wild-type protein (80.5 °C) and the E34D mutant (72.7 °C) at pH 7.0 and 20 μM protein concentration described elsewhere [4,18]. These T_m values are still high at pH 4.00 and even at 3.75 (73.2 °C and 69.2 °C at pH 4.00, and 69.0 °C and 65.2 °C at pH 3.75 for the wild-type and the mutant, respectively, as recalculated from Table 1 for a 20 μM concentration). The large destabilization of the native structure, as clearly seen in both the T_m and ΔG_U values (Table 1) when pH decreases by only 0.25 units from 3.75 to 3.50, indicates that most of the structurally important acid groups lose their charge in this pH range, thus leaving the positively charged clusters uncompensated. Among these acid groups the presence of the Glu34 side chain in an optimum strategic position and orientation within a relatively large cluster dominated by positively charged groups (each of the two symmetrical clusters includes A-K13, A-R9, A-K12, the N-terminal amino group of chain A, B-K38, B-E34 and B-E40, where A and B refer to the two chains of the homodimer) would clearly decrease electrostatic repulsion and probably stabilize the folded conformation more efficiently than does the shorter chain of the Asp residue in the E34D mutant [4,18].

Furthermore, the $\Delta\Delta G$-values in Table 1 decrease sharply from pH 3.75 to pH 3.50 and the 4 °C difference in T_m between the wild-type and the E34D mutant at both pH 4.00 and 3.75 decreases to only 2 °C at pH 3.50. These values, together with the fact that in HU*Bst*, in which the Glu34-Lys13 salt–bridge interaction cannot exist, the difference in T_m at pH 7.0 is in the region of 2 °C, as compared to 7.8 °C for HU*Tmar* also at pH 7.0 [4,18] again supports the importance to thermostability not only of electrostatic interactions but particularly that of the above salt bridge, which breaks down in wild-type HU*Tmar* on the protonation of Glu34 at pH 3.50. In fact, the significant contribution of ion pairs to stability has recently been described in other hyperthermophilic proteins from *T. maritima* [37,39] (see [40] for a review). An examination of the unfolding entropy changes would lead to similar conclusions. Thus, for example, the $\Delta\Delta S_{U,25}$ values at 25 °C corresponding to those of $\Delta\Delta G_{U,25}$ in Table 1 are −6.0, −5.5 and −2.0 J·K^{-1}·mol^{-1} at pH 4.00, 3.75 and 3.50, respectively, and, given the known 'entropic character' of electrostatic interactions, salt bridges for example, both the sign and trend of these entropy values fit in with our interpretation, and with the above comments on the entropic contribution to ΔG_U in Fig. 7.

One other important observation is that when pH is lowered to 3.50 the native structure of HU*Tmar* destabilizes to such an extent that it becomes possible to unfold it at low temperature simply by decreasing the protein concentration within experimental limits (Fig. 6). Fig. 5B also shows how the θ_{222} value of the 30 μM concentration of wild-type protein at pH 3.50 does not reach the value corresponding to the 100% folded population at 20 °C (around −13 000 deg·cm^2·dmol^{-1}), because the closeness of cold denaturation precludes the protein's folding completely at low temperatures. This concentration-dependent unfolding process, as monitored by CD, follows precisely the transition curves obtained using DSC thermodynamic data (Figs 5B and 6B). All this, together with the existence of an isosbestic point on the CD spectra (Fig. 6A), confirms the correctness of the two-state dissociation/unfolding model and further suggests that the DNA-binding arms do not contribute appreciably to the co-operative unfolding of the histone core. It should be mentioned at this juncture, however, that although the thermal unfolding of the HU proteins studied so far has always been considered to be a two-state process [4,15,22–24,41], it has been proposed very recently that the denaturation of some mesophilic HU proteins from *Escherichia coli* at pH 7.4 is a biphasic, three-state process [42].

Finally, from all the above, we conclude that optimized electrostatic interactions, the effects of which decrease less with temperature than those of other structural factors such as the hydrophobic effect, and also lead to a low heat capacity of unfolding, contribute significantly to the very high thermal stability of the HU*Tmar* protein.

Acknowledgements

This work was supported by grants BIO4-96-0670 from the European Union and BIO2000-1459 and BIO2003-04274 from the Spanish Ministry of Science and Technology. V. V. F. was supported by RFBR (Russian Federation) Grant 03-04-48331. We thank our colleagues Dr J.C. Martinez and Dr F. Conejero for their helpful suggestions and Dr J. Trout for revising the English text.

References

1. McCrary, B.S., Edmondson, S.P. & Shriver, J.W. (1996) Hyperthermophile protein folding thermodynamics: Differential scanning calorimetry and chemical denaturation of Sac7d. *J. Mol. Biol.* **264**, 784–805.
2. Jaenicke, R. & Böhm, G. (1998) The stability of proteins in extreme environments. *Curr. Opin. Struct. Biol.* **8**, 738–748.
3. Szilagyi, A. & Zavodsky, P. (2000) Structural differences between mesophilic, moderately thermophilic and extremely thermophilic protein subunits: results of comprehensive survey. *Struct. Fol. Des.* **8**, 493–504.
4. Christodoulou, E. & Vorgias, C.E. (2002) The thermostability of DNA-binding protein HU from mesophilic, thermophilic and extreme thermophilic bacteria. *Extremophiles* **6**, 21–31.
5. Menendez-Arias, L. & Argos, P. (1989) Engineering protein thermal stability. Sequence statistics point to residue substitutions in α-helices. *J. Mol. Biol.* **206**, 397–406.
6. Akanuma, S., Yamagishi, A., Tanaka, N. & Oshima, T. (1998) Serial increase in the thermal stability of IPMDH from *Bacillus subtilis* by experimental evolution. *Protein Sci.* **7**, 678–705.
7. Esser, D., Rudolph, R., Jaenicke, R. & Böhm, G. (1999) The HU protein from *Thermotoga maritima*: Recombinant expression, purification and physicochemical characterization of an extremely hyperthermophilic DNA-binding protein. *J. Mol. Biol.* **291**, 1135–1146.
8. Hollien, J. & Marqusee, S. (1999) A thermodynamic comparison of mesophilic and thermophilic ribonucleases H. *Biochemistry* **38**, 3831–3836.
9. Kumar, S., Tsai, C.J. & Nussinov, R. (2001) Thermodynamic differences among homologous thermophilic and mesophilic proteins. *Biochemistry* **40**, 14152–14165.
10. Drlica, K. & Rouviere-Yaniv, J. (1987) Histonelike proteins of bacteria. *Microbiol. Rev.* **51**, 301–319.
11. Hwang, D.S. & Kornberg, A. (1992) Opening of the replication origin of *Escherichia coli* by DnaA protein with protein HU or IHF. *J. Biol. Chem.* **267**, 23083–23086.
12. Lavoie, B.D. & Choconas, G. (1994) A second high affinity HU bending site in the phage Mu transpososome. *J. Biol. Chem.* **269**, 15571–15576.
13. Castaing, B., Zelwer, C., Laval, J. & Boiteux, S. (1995) HU protein of *Escherichia coli* binds specifically to DNA that contains single-strand breaks or gaps. *J. Biol. Chem.* **270**, 10291–10296.
14. Kamashev, D. & Rouvière-Yaniv, J. (2000) The histone-like protein HU binds specifically to DNA recombination and repair intermediates. *EMBO J.* **23**, 6527–6535.
15. Wilson, K.S., Vorgias, C.E., Tanaka, I., White, S.W. & Kimura, M. (1990) The thermostability of DNA-binding protein HU from Bacilli. *Protein Eng.* **4**, 11–22.
16. Padas, P.M., Wilson, K.S. & Vorgias, C.E. (1992) The DNA-binding protein HU from mesophilic and thermophilic bacilli: gene cloning, overproduction and purification. *Gene* **117**, 39–44.
17. Christodoulou, E. & Vorgias, C.E. (1998) Cloning, over-production, purification and crystallization of the DNA binding protein HU from hyperthermophilic eubacterium *Thermotoga maritima*. *Acta Cristallogr. D Biol. Crystallogr.* **54**, 1043–1045.
18. Christodoulou, E., Rypniewski, W.R. & Vorgias, C.E. (2003) High-resolution X-ray structure of the DNA-binding protein HU from the hyperthermophilic *Thermotoga maritima* and the determinants of its thermostability. *Extremophiles* **7**, 111–122.
19. White, S.W., Appelt, K., Wilson, K.S. & Tanaka, I. (1989) A protein structural motif that bends DNA. *Proteins Struct. Funct. Genet.* **5**, 281–288.
20. Vis, H., Mariani, M., Vorgias, C.E., Wilson, K.S., Kaptein, R. & Boelens, R. (1995) Solution structure of the HU protein from *Bacillus stearothermophilus*. *J. Mol. Biol.* **254**, 692–703.
21. White, S.W., Wilson, K.S., Appelt, K. & Tanaka, I. (1999) The high-resolution structure of DNA-binding protein HU from *Bacillus stearothermophilus*. *Acta Crystallogr. D* **55**, 801–809.
22. Kawamura, S., Kakuta, Y., Tanaka, I., Hikichi, K., Kuhara, S., Yamasaki, N. & Kimura, M. (1996) Glycine-15 in the bend between two-helices can explain the thermostability of DNA binding protein HU from *Bacillus stearothermophilus*. *Biochemistry* **35**, 1195–1200.
23. Kawamura, S., Tanaka, I., Yamasaki, N. & Kimura, M. (1997) Contribution of a salt bridge to the thermostability of DNA binding protein HU from *Bacillus stearothermophilus* determined by site-directed mutagenesis. *J. Biochem. (Tokyo)* **121**, 448–455.
24. Kawamura, S., Abe, Y., Ueda, T., Masumoto, K., Imoto, T., Yamasaki, N. & Kimura, M. (1998) Investigation of the structural basis for thermostability of DNA binding protein HU from *Bacillus stearothermophilus*. *J. Biol. Chem.* **273**, 19982–19987.
25. Gill, S.C. & von Hippel, P.H. (1989) Calculation of protein extinction coefficients from amino acid sequence data. *Anal. Biochem.* **182**, 319–326.
26. Ruiz-Sanz, J., Simoncsits, A., Törö, I., Pongor, S., Mateo, P.L. & Filimonov, V.V. (1999) A thermodynamic study of the 434-repressor N-terminal domain and of its covalently linked dimmers. *Eur. J. Biochem.* **263**, 246–253.
27. Makhatadze, G.I. & Privalov, P.L. (1990) Heat capacity of proteins. I. Partial molar heat capacity of individual amino acid residues in aqueous solutions: hydration effect. *J. Mol. Biol.* **213**, 375–384.
28. Nojima, H., Ikai, A., Oshima, T. & Noda, H. (1977) Reversible thermal unfolding of thermostable phosphoglycerate kinase. Thermostability associated with mean zero enthalpy change. *J. Mol. Biol.* **116**, 429–442.
29. Privalov, P.L. (1979) Stability of proteins. Small globular proteins. *Adv. Protein Chem.* **33**, 167–241.
30. Cobos, E.S., Filimonov, V.V., Galvez, A., Maqueda, M., Valdivia, E., Martinez, J.C. & Mateo, P.L. (2001) AS-48: a circular protein with an extremely stable globular structure. *FEBS Lett.* **505**, 379–382.
31. Schuler, B., Kremer, W., Kalbitzer, H.R. & Jaenicke, R. (2002) Role of entropy in protein thermostability: Folding kinetics of a hyperthermophilic cold shock protein at high temperatures using ^{19}F NMR. *Biochemistry* **41**, 11670–11680.
32. Kumar, S., Tsai, C.J. & Nussinov, R. (2003) Temperature range of thermodynamic stability for the native state of reversible two-state proteins. *Biochemistry* **42**, 4864–4873.
33. Alexander, P., Fahnestock, S., Lee, T., Orban, J. & Bryan, P. (1992) Thermodynamic analysis of the folding of the streptococcal protein G IgG-binding domains B1 and B2: why small proteins tend to have high denaturation temperatures. *Biochemistry* **31**, 3597–3603.
34. Murphy, K.P. & Freire, E. (1992) Thermodynamics of structural stability and cooperative folding behaviour in proteins. *Adv. Protein Chem.* **43**, 313–361.
35. Zhou, H.-X. (2002) Toward the physical basis of thermophilic proteins: Linking of enriched polar interactions and reduced heat capacity of unfolding. *Biophys. J.* **83**, 3126–3133.

36. Zhou, H.-X. & Dong, F. (2003) Electrostatic contributions to the stability of a thermophilic cold shock protein. *Biophys. J.* **84**, 2216–2222.
37. Karshikoff, A. & Ladenstein, R. (2001) Ion pairs and the thermotolerance of proteins from hyperthermophiles: a 'traffic rule' for hot roads. *Trends Biochem. Sci.* **26**, 550–556.
38. Filimonov, V.V., Pfeil, W., Tsalkova, T.N. & Privalov, P.L. (1978) Thermodynamic investigations of proteins. IV. calcium binding protein parvalbumin. *Biophys. Chem.* **8**, 117–122.
39. Lebbink, J.H.G., Consalvi, V., Chiaraluce, R., Berndt, K.D. & Ladenstein, R. (2002) Structural and thermodynamic studies on a salt-bridge triad in the NADP-binding domain of glutamate dehydrogenase from *Thermotoga maritima*: Cooperativity and electrostatic contribution to stability. *Biochemistry* **41**, 15524–15535.
40. Jaenicke, R. & Böhm, G. (2001) Thermostability of proteins from *Thermotoga maritima*. *Methods Enzymol.* **334**, 438–469.
41. Welfle, H., Misselwitz, R., Welfle, K., Schindelin, H., Scholtz, A.S. & Heinemann, U. (1993) Conformations and conformational changes of four Phe→Trp variants of the DNA-binding histone-like protein, HBsu, from *Bacillus subtilis* studied by circular dichroism and fluorescence spectroscopy. *Eur. J. Biochem.* **217**, 849–856.
42. Ramstein, J., Hervouet, N., Coste, F., Zelwer, C., Oberto, J. & Castaing, B. (2003) Evidence of a thermal unfolding dimeric intermediate for the *Escherichia coli* histone-like HU proteins: Thermodynamics and structure. *J. Mol. Biol.* **331**, 101–121.

Appendix

Fitting of the DSC curves to the two-state dissociation/unfolding model

Subroutine for a single Cp curve.
Independent variable: T (K)
Dependent variable: C_p (kJ·K^{-1}·mol^{-1})
Parameters
Fixed: b_U, c_U, C_t
Adjustable: a_N, b_N, a_U, T_m, $\Delta H_{U,m}$
Equations

$$R = 0.008314$$

$$C_{p,N2} = a_N + b_N \cdot T$$

$$C_{p,U} = a_U + b_U \cdot T + c_U \cdot T^2$$

$$\Delta C_{p,U} = C_{p,U} - C_{p,N2}$$

$$\Delta H_U = \Delta H_{U,m} + \int_{T_m}^{T} \Delta C_{p,U} \cdot dT$$

$$\Delta H_U = \Delta H_{U,m} + (a_U - a_N)\cdot(T - T_m) + \frac{(b_U - b_N)}{2}\cdot(T^2 - T_m^2) + \left(\frac{c_U}{3}\right)\cdot(T^3 - T_m^3)$$

$$\Delta S_U = \Delta S_{U,m} + \int_{T_m}^{T} \frac{\Delta C_{p,U}}{T}\cdot dT = \frac{\Delta H_{U,m}}{T_m} + 0.5\cdot R\cdot\ln(C_t) + \int_{T_m}^{T} \frac{\Delta C_{p,U}}{T}\cdot dT$$

$$\Delta S_U = \frac{\Delta H_{U,m}}{T_m} + 0.5\cdot R\cdot\ln(C_t) + (a_U - a_N)\cdot\ln\left(\frac{T}{T_m}\right) + (b_U - b_N)\cdot(T - T_m) + \left(\frac{c_U}{2}\right)\cdot(T^2 - T_m^2)$$

$$\Delta G_U = \Delta H_U - T\cdot\Delta S_U$$

$$K_U = \exp\left(\frac{-\Delta G_U}{R\cdot T}\right)$$

$$X_U = \left(\frac{K_U}{4C_t}\right)\cdot\left(-K_U + \sqrt{K_U^2 + 8C_t}\right)$$

$$C_p = C_{p,N2} + X_U\cdot\Delta C_{p,U} + \frac{2\Delta H_U^2\cdot X_U\cdot(1 - X_U)}{(2 - X_U)\cdot R\cdot T^2}$$

Subroutine for multiple Cp curves at different concentrations for the same protein sample.
Independent variable: T (K)
Dependent variable: C_p (kJ·K^{-1}·mol^{-1}) (one per each C_p curve)
Parameters
Fixed for all traces: b_U, c_U, $C_{t,ref}$
Fixed for each trace: C_t
Adjustable for all traces: a_N, b_N, a_U, T_m, $\Delta H_{U,m}$
Equations
Here T_m and $\Delta H_{U,m}$ are referred to a reference concentration (120 μM), $C_{t,ref}$, and the enthalpy function is common for all curves as described in Materials and methods. All equations are the same as the previous ones except that of ΔS_U, which is expressed in terms of $C_{t,ref}$;

$$\Delta S_U = \Delta S_{U,m} + \int_{Tm}^{T} \frac{\Delta C_{p,U}}{T}\cdot dT$$

$$\Delta S_U = \frac{\Delta H_{U,m}}{T_m} + 0.5\cdot R\cdot\ln(C_{t,ref}) + (a_U - a_N)\cdot\ln\left(\frac{T}{T_m}\right) + (b_U - b_N)\cdot(T - T_m) + \left(\frac{c_U}{2}\right)\cdot(T^2 - T_m^2)$$

Subroutine for multiple Cp curves at different concentrations, different pH values and different protein samples.
Independent variable: T (K)
Dependent variable: C_p (kJ·K^{-1}·mol^{-1}) (one per each C_p curve)
Parameters
Fixed for all traces: b_U, c_U
Fixed for each trace: C_t
Adjustable for all traces: a_N, b_N, a_U, T_{ref}, $\Delta H_{U,ref}$
Adjustable for each pH value and protein sample: $K_{U,ref}$
To fit the DSC curves at different concentrations for different pH conditions and different protein samples, it was assumed that the unfolding enthalpy depends upon temperature but not on pH or protein sample. That is, we use here the same unfolding enthalpy function for the two protein samples at the three pH values investigated. In this case, we can express ΔH_U, ΔS_U and ΔG_U in terms of a reference temperature (for example, 298.15 K), T_{ref}. In this way, the equations for the fitting are the following:
Equations

$$R = 0.008314$$

$$C_{p,N2} = a_N + b_N\cdot T$$

$$C_{p,U} = a_U + b_U\cdot T + c_U\cdot T^2$$

$$\Delta C_{p,U} = C_{p,U} - C_{p,N2}$$

$$\Delta H_U = \Delta H_{U,ref} + \int_{T_{ref}}^{T} \Delta C_{p,U} \cdot dT$$

$$\Delta H_U = \Delta H_{U,ref} + (a_U - a_N)\cdot(T - T_{ref}) + \frac{(b_U - b_N)}{2}\cdot(T^2 - T_{ref}^2) + \left(\frac{c_U}{3}\right)\cdot(T^3 - T_{ref}^3)$$

$$\Delta S_U = \Delta S_{U,ref} + \int_{T_{ref}}^{T} \frac{\Delta C_{p,U}}{T}\cdot dT = \frac{\Delta H_{U,ref}}{T_{ref}} + R\cdot\ln(K_{U,ref}) + \int_{T_{ref}}^{T} \frac{\Delta C_{p,U}}{T}\cdot dT$$

$$\Delta S_U = \frac{\Delta H_{U,ref}}{T_{ref}} + R\cdot\ln(K_{U,ref}) + (a_U - a_N)\cdot\ln\left(\frac{T}{T_{ref}}\right) + (b_U - b_N)\cdot(T - T_{ref}) + \left(\frac{c_U}{2}\right)\cdot(T^2 - T_{ref}^2)$$

$$\Delta G_U = \Delta H_U - T\cdot\Delta S_U$$

$$K_U = \exp\left(\frac{-\Delta G_U}{R\cdot T}\right)$$

$$X_U = \left(\frac{K_U}{4C_t}\right)\cdot\left(-K_U + \sqrt{K_U^2 + 8C_t}\right)$$

$$C_p = C_{p,N2} + X_U\cdot\Delta C_{p,U} + \frac{2\Delta H_U^2\cdot X_U\cdot(1 - X_U)}{(2 - X_U)\cdot R\cdot T^2}$$

Fitting of the CD thermal curves to the two-state dissociation/unfolding model

The heat capacity change upon unfolding, $\Delta C_{p,U}$, used here was that obtained in the DSC fittings.

Subroutine for a single CD curve.
Independent variable: T (K)
Dependent variable: θ_{222} (deg·cm^2·dmol^{-1})
Parameters
Fixed: a_N, b_N, a_U, b_U, c_U, C_t
Adjustable: $\theta_{N2,a}$, $\theta_{N2,b}$, $\theta_{U,a}$, $\theta_{U,b}$, T_m, $\Delta H_{U,m}$
Equations

$$R = 0.008314$$

$$C_{p,N2} = a_N + b_N\cdot T$$

$$C_{p,U} = a_U + b_U\cdot T + c_U\cdot T^2$$

$$\Delta C_{p,U} = C_{p,U} - C_{p,N2}$$

$$\Delta H_U = \Delta H_{U,m} + (a_U - a_N)\cdot(T - T_m) + \frac{(b_U - b_N)}{2}\cdot(T^2 - T_m^2) + \left(\frac{c_U}{3}\right)\cdot(T^3 - T_m^3)$$

$$\Delta S_U = \frac{\Delta H_{U,m}}{T_m} + 0.5\cdot R\cdot\ln(C_t) + (a_U - a_N)\cdot\ln\left(\frac{T}{T_m}\right) + (b_U - b_N)\cdot(T - T_m) + \left(\frac{c_U}{2}\right)\cdot(T^2 - T_m^2)$$

$$\Delta G_U = \Delta H_U - T\cdot\Delta S_U$$

$$K_U = \exp\left(\frac{-\Delta G_U}{R\cdot T}\right)$$

$$X_U = \left(\frac{K_U}{4C_t}\right)\cdot\left(-K_U + \sqrt{K_U^2 + 8C_t}\right)$$

$$C_p = C_{p,N2} + X_U\cdot\Delta C_{p,U} + \frac{2\Delta H_U^2\cdot X_U\cdot(1 - X_U)}{(2 - X_U)\cdot R\cdot T^2}$$

$$\theta_{N2} = \theta_{N2,a} + \theta_{N2,b}\cdot T$$

$$\theta_U = \theta_{U,a} + \theta_{U,b}\cdot T$$

$$\theta_{222} = \theta_{N2} + X_U\cdot(\theta_U - \theta_{N2})$$

Multiple fittings were performed in a similar way as in the DSC fittings.

Fitting of the concentration dependence of the CD signal at a constant, working temperature, T_w, to the two-state dissociation/unfolding model

Here we have used the corresponding $K_{U,w}$-value obtained by the multiple DSC curves fitting.

Subroutine.
Independent variable: C_t (mol of monomer)
Dependent variable: θ_{222} (deg·cm^2·dmol^{-1})
Parameters
Fixed: $K_{U,w}$
Adjustable: $\theta_{N2,w}$, $\theta_{U,w}$
Equations

$$X_U = \left(\frac{K_{U,w}}{4C_t}\right)\cdot\left(-K_{U,w} + \sqrt{K_{U,w}^2 + 8C_t}\right)$$

$$\theta_{222} = \theta_{N2,w} + X_U\cdot\left(\theta_{U,w} - \theta_{N2,w}\right)$$